Response of CO_2 and H_2O fluxes of a mountainous tropical rainforest in equatorial Indonesia to El Niño events

A. Olchev[1,2], A. Ibrom[3], O. Panferov[4], D. Gushchina[5], H. Kreilein[2], V. Popov[6,7], P. Propastin[2], T. June[8], A. Rauf[9], G. Gravenhorst[*] and A. Knohl[2]

[1] {A.N. Severtsov Institute of Ecology and Evolution of RAS, Moscow, Russia}
[2] {Department of Bioclimatology, Faculty of Forest Sciences and Forest Ecology, Georg-August University of Goettingen, Goettingen, Germany}
[3] {Centre for Ecosystems and Environmental Sustainability, Department of Chemical and Biochemical Engineering, Technical University of Denmark, Roskilde, Denmark}
[4] {Climatology and Climate Protection, Faculty of Life Sciences and Engineering, University of Applied Sciences, Bingen am Rhein, Germany}
[5] {Department of Meteorology and Climatology, Faculty of Geography, Moscow State University, Moscow, Russia}
[6] **{**Faculty of Physics, Lomonosov Moscow State University, Moscow, Russia**}**
[7] {Financial University under the Government of the Russian Federation, Moscow, Russia}
[8] { Bogor Agricultural University, Department of Geophysics and Meteorology}
[9] {Universitas Tadulako, Palu, Indonesia}
[*] {Retired}

Correspondence to: A. Olchev (aoltche@gmail.com)

Abstract

The possible impact of El Niño-Southern Oscillation (ENSO) events on the main components of CO_2 and H_2O fluxes between tropical rainforest and atmosphere is investigated. The fluxes were continuously measured in a pristine mountainous tropical rainforest growing in Central Sulawesi in Indonesia using the eddy covariance method for the period from January 2004 to June 2008. During this period, two episodes of El Niño and one episode of La Niña were observed. All these ENSO episodes had moderate intensity and were of Central Pacific type. The temporal variability analysis of the main meteorological parameters and components of CO_2 and H_2O exchange showed a high sensitivity of Evapotranspiration (ET) and Gross Primary Production (GPP) of the tropical rainforest to meteorological variations caused by both El Niño and La Niña episodes. Incoming solar radiation is the main governing factor that is responsible for ET and GPP

variability. Ecosystem Respiration (RE) dynamics depend mainly on the air temperature changes and are almost insensitive to ENSO. Changes of precipitation due to moderate ENSO events did not cause any notable effect on ET and GPP, mainly because of sufficient soil moisture conditions even in periods of anomalous reduction of precipitation in the region.

1. Introduction

The contribution of tropical rainforests to the global budget of greenhouse gases, their possible impact on the climatic system, and their sensitivity to climatic changes are key topics of numerous theoretical and experimental studies (Clark and Clark, 1994; Grace et al., 1995, 1996; Malhi et al., 1999; Ciais et al., 2009; Lewis et al., 2009; Phillips et al., 2009; Malhi, 2010; Fisher et al., 2013; Moser et al., 2014). The area covered by tropical rainforests was drastically reduced during the last century, mainly due to human activities and presently there are less than 11.0 million km^2 remaining (Malhi, 2010). While deforestation rates in the tropical forests of Brazil are now declining, countries in South-East Asia, particularly Indonesia, show globally the largest increase in forest loss (Hansen et al., 2013), resulting in major changes in carbon and water fluxes between the land surface and the atmosphere. Therefore, during the last decade the tropical forest ecosystems of South-East Asia and especially Indonesia are the focus area of intensive studies of biogeochemical cycle and land surface - atmosphere interactions. On the one hand, it is necessary to know how these tropical forests influence the global and regional climate, and on the other hand, how they respond to changes of regional climatic conditions.

Climate and weather conditions in the equatorial Pacific and South-Eastern part of Asia are mainly influenced by the Intertropical Convergence Zone (ITCZ) which is seasonally positioned north and south of the equator. Another very important factor affecting the climate of South-East Asia is the well-known coupled oceanic and atmospheric phenomenon, El Niño-Southern Oscillation (ENSO). During the warm phase of ENSO, termed "El Niño", sea surface temperature (SST) in the central and eastern parts of the equatorial Pacific sharply increases, and during a cold phase of the phenomenon, termed "La Niña", the SST in these areas is lower than usual. Both phenomena, El Niño and La Niña, lead to essential changes of pressure distribution and atmospheric circulation and, as a result, to anomalous changes of precipitation amount, solar radiation, and temperature fields, both in the regions of sea surface temperature anomalies and in a wide range of remote areas through the mechanism of atmospheric bridges (Wang, 2002; Graf and Zanchettin, 2012). Typically, in Indonesia El Niño results in dryer conditions and La Niña results in wetter conditions, potentially impacting the land vegetation (Erasmi et al., 2009). ENSO events are irregular, characterised by different intensity and, are usually observed at intervals of 2-7 years.

To describe the possible effects of ENSO events on CO_2 and H_2O exchange between land surface and the atmosphere, many studies for different Western Pacific regions were carried out during recent decades (Feely et al., 1998; Malhi et al., 1999; Rayner and Law, 1999; Aiba and Kitayama, 2002; Hirano et al., 2007; Erasmi et al., 2008; Gerold and Leemhuis, 2010). They are mainly based on the results of modelling experiments and remote sensing data (Rayner and Law, 1999). Experimental results based on direct measurements of CO_2 and H_2O fluxes, which allow studying the response of individual terrestrial ecosystems to anomalous weather conditions, are still very limited (e.g. Hirano et al., 2007; Moser et al., 2014). Existing monitoring networks in equatorial regions of the Western Pacific are associated mainly with lowland areas and do not cover mountainous rainforest regions, even though mountainous regions cover some of the last remaining undisturbed rainforest in South-East Asia. Most attention in former studies was paid to the description of plant response to anomalously dry and warm weather during El Niño events (Aiba and Kitayama, 2002; Hirano et al., 2007; Moser et al., 2014). The possible changes in plant functioning during La Niña events are still not clarified. In particular, Malhi et al. (1999) reported that for Amazon region in the South America El Niño periods are strongly associated with enhanced dry seasons that probably result in increased carbon loss, either through water stress causing reduced photosynthesis or increased tree mortality. Aiba and Kitayama (2002) examined the effects of the 1997–98 El Niño drought on nine rainforests of Mount Kinabalu in Borneo using forest inventory and showed that El Niño increased the tree mortality for lowland forests. However, it did not affect the growth rate of the trees of upland forests (higher than 1,700 m) where mortality was restricted by some understorey species only. Eddy covariance measurements of the CO_2 fluxes in a tropical peat swamp forest in Central Kalimantan, Indonesia, for the period from 2002 to 2004, provided by Hirano et al. (2007), showed that during the El Niño event in the period November-December 2002 the annual net CO_2 release reached maximal values, mainly due to strong decrease of GPP in the late dry season, because of dense smoke emitted from large-scale fires. Effects of El Niño on annual RE in 2002 were insignificant.

There is a lack of experimental data on CO_2 and H_2O fluxes in mountainous rainforests in equatorial regions of the Western Pacific, and on their response to ENSO. Hence, the main objective of this study was to evaluate and quantify the impact of ENSO events on the main components of CO_2 and H_2O fluxes in a pristine mountainous tropical rainforest growing in Central Sulawesi, Indonesia. The methodology used was analysis of long-term eddy covariance flux measurement data.

2. Materials and Methods

2.1 El Niño's types and intensity

Nowadays, two types of ENSO can be distinguished: 1) the canonical or conventional El Niño, which is characterised by SST anomalies located in the eastern Pacific near the South American coast (Rasmusson and Carpenter, 1982) and 2) the Central Pacific El Niño or El Niño Modoki (Larkin and Harrison, 2005; Ashok et al., 2007; Kug et al., 2009; Ashok and Yamagata, 2009; Gushchina and Dewitte, 2012). In 2003, the new definition of the conventional El Niño was accepted by the National Oceanic and Atmospheric Administration (NOAA) of the USA, in referring to the warming of the Pacific region between 5°N - 5°S and 170° - 120°W. According to Ashok et al. (2007) the Central Pacific El Niño/El Niño Modoki - i.e. unusually high SST - occurs roughly in the region between 160°E - 140°W and 10°N - 10°S.

As criteria to assess the intensity of ENSO events, a wide range of indexes based on different combinations of sea level pressure and SST data in various areas of the Pacific are used. For diagnostics of the central Pacific El Niño, the SST anomalies (in °C) in Nino4 region (5°N - 5°S and 160°E - 150°W) are broadly used (Figure 1). The monthly SST anomalies (in °C) in Nino3.4 region (5°N - 5°S and 170° - 120°W) are used to diagnose both types of El Niño phenomenon: canonical and Central Pacific (Download Climate Timeseries, 2013).

2.2 Experimental site

The tropical rainforest selected for the study is situated near the village Bariri in the southern part of the Lore Lindu National Park of Central Sulawesi in Indonesia (1°39.47'S and 120°10.409'E or UTM 51S 185482 м east and 9816523 м north) (Figure 1). The site is located on a large plateau of several kilometres in size at about 1,430 m above sea level surrounded by mountain chains surmounting the plane by another 300 m to 400 m. Within 500 m around the tower the elevation varies between 1,390 and 1,430 metres. Wind field measurement with a sonic anemometer indicate a slope of around 2-3°, which is similar to many Fluxnet sites. About 1,000 m to the east from the experimental site, the forest is replaced by a meadow; in all other directions the forest extends several kilometres.(Ibrom et al., 2007).

According to the Köppen climate classification the study area relates to tropical rainforest climate (*Af*) (Chen D. and Chen H.W., 2013). Weather conditions of the region are mainly influenced by the ITCZ. During the wet season (typically, from November to April) the area is influenced by very moist northeast monsoons coming from the Pacific. Maximum precipitation during the observation period from January 2004 to July 2008 was observed in April - with 258.0±148.0 mm month^{-1}. The drier season usually lasts from May to October. The precipitation minimum was observed in September with 195.0±48.0 mm month^{-1}. The September-October period was also characterised by maximal incoming solar radiation, up to 650±47.0 MJ m^{-2} $month^{-1}$, mainly because of a significant decrease of convective clouds, due to the reversing of oceanic northeast monsoon to a southeast monsoon blowing from the Australian continent. The mean annual precipitation amount exceeded 2000 mm. The mean monthly air temperature varies between 19.4 and 19.7 °C. The mean annual air temperature was 19.5 °C (Falk et al., 2005; Ibrom et al., 2007).

The vegetation at the experimental site is very diverse and represented by more than 88 different tree species per hectare. Among the dominant species are *Castanopsis accuminatissima* BL. (29%), *Canarium vulgare* Leenh. (18%) and *Ficus spec.* (9.5%). The density of trees, with diameter at breast height larger than 0.1 m, is 550 trees per ha. In addition, there is more than a 10-fold larger number of smaller trees per hectare with stem diameter lower than 0.1 m. The total basal area of trees reached 53 m^2 per ha. Leaf area index (LAI) is about 7.2 m^2 m^{-2}. LAI has been estimated using an indirect hemispherical photography approach with a correction for leaf clumping effects. The height of the trees, with diameters at breast height larger than 0.1 m, varies between the lowest at 12 m and the highest at 36 m. The mean tree height is 21 m (Ibrom et al., 2007).

2.3 Flux measurements

CO_2 and H_2O fluxes were measured from 2004 to 2008 within the framework of the STORMA project (Stability of Rainforest Margins in Indonesia, SFB 552), supported by the German Science Foundation (DFG). The eddy covariance equipment for flux measurement was installed on a meteorological tower of 70 m height at the 48 m level, i.e. ca. 12 m higher than the maximal tree height. The measuring system consists of a three-dimensional sonic anemometer (USA-1, Metek, Germany) and an open-path CO_2 and H_2O infrared gas analyzer (IRGA, LI-7500, Li-Cor, USA) (Falk et al., 2005; Ibrom et al., 2007; Panferov et al., 2009). The open-path IRGA was calibrated with calibration gases two times per year and showed no considerable sensitivity drift within one year of operation. Turbulence data were sampled at 10 Hz and stored as raw data on an industrial mini PC (Kontron, Germany). All instruments were powered by batteries, which were charged by solar panels, mounted on the tower. The system is entirely self-sustaining and has been proven to run unattended over a period of several months. Post-field data processing on eddy covariance flux estimates was carried out strictly according to the established recommendations for data analysis (Aubinet et al., 2012). In addition to the procedures described in Falk et al. (2005) and Ibrom et al. (2007), we corrected the flux data for CO_2 or H_2O density fluctuations due to heat conduction from the open-path sensor (Burba et al., 2008; Järvi et al. 2009) using finally the suggested method as described in Reverter et al. (2011).

The system operated at ca. 70% of the time. Ca. 30% of the measured flux data were negatively affected by rain and other unfavourable conditions and removed. From night time ecosystem respiration data a friction velocity (u_*) threshold value of 0.25 m s^{-1} was estimated (Aubinet et al., 2000), i.e. at u_* values above this threshold the measured night time flux became independent from u_*. Night time flux values that were measured at $u_* < 0.25$ m s^{-1} were removed, which left 15% of the measured night time flux data in the data set. For filling the gaps in the measured Net Ecosystem Exchange (NEE) data, as well as the gaps in net radiation, sensible and latent heat flux records the process-based Mixfor-SVAT model (Olchev et al., 2002; 2008) were applied. The Mixfor-SVAT model was also used to quantify RE and forest canopy transpiration. The model was validated using long-term data records obtained for the tropical rainforest in Bariri under well-developed turbulent conditions. The results of model validation showed a good agreement of model calculations with field observations for a broad spectrum of weather and soil moisture conditions (Falk et al., 2005; Falge et al., 2005; Olchev et al., 2008). GPP of the tropical rainforest was derived as a difference between measured NEE and RE.

2.4 Micrometeorological measurements

Air temperature, relative humidity and horizontal wind speed were measured at 4 levels above and at 2 levels inside the forest canopy using ventilated and sheltered thermo-hygrometers and cup anemometers (Friedrichs Co., Germany) installed on the tower. Short- and long-wave radiation components were measured below and above the canopy with CM6B and CG1 sensors (Kipp & Zonen, The Netherlands). Rainfall intensity was measured on top of the tower with a tipping bucket in a Hellman-type rain gauge. To fill the gaps in measuring records the meteorological data from an autonomic meteorological station, situated about 900 m away from the tower outside the forest on a nearby meadow, were used. For the analysis, the monthly mean values of air temperature and monthly sums of precipitation and solar energy were calculated.

2.5 Data analysis

To estimate the possible impact of ENSO events on CO_2 and H_2O fluxes in the tropical rainforest at Bariri the temporal variability of monthly NEE, GPP, RE and ET in periods with different ENSO intensity was analysed. To quantify the ENSO impacts on meteorological parameters and fluxes and to distinguish them from effects caused by the seasonal migration of the ITCZ, the intra-annual patterns of CO_2 and H_2O fluxes as well as meteorological conditions during the measuring period were also evaluated.

In the first step to assess the possible impact of ENSO events on meteorological parameters (global solar radiation (G), precipitation amount (P), air temperature (T) and CO_2 and H_2O fluxes, the correlation between the absolute values of monthly G, P, T, NEE, GPP, RE, ET and monthly SST-anomalies in Nino4 and Nino3.4 regions (Nino4 and Nino3.4 indexes) were analysed.

In the second step we analyzed the correlation between the deviations of monthly meteorological parameter and flux values from their monthly averages over the entire measuring period and the Nino4/Nino3.4 indexes.. The deviation in the case of GPP (ΔGPP) was estimated as

$$\Delta GPP_{Month,Year} = GPP_{Month,Year} - \frac{1}{N}\sum_{Year=2004}^{2008} GPP_{Month,Year}$$

where $GPP_{Month,Year}$ is total monthly GPP for a particular month (January to December) and corresponding year (2004 to 2008), $\frac{1}{N}\sum_{Year=2004}^{2008} GPP_{Month,Year}$ is monthly GPP for this particular month averaged for the entire measuring period (2004 to 2008); N is number of years. Positive values in ΔGPP, ΔRE, and ΔNEE indicate GPP, RE higher and NEE (carbon uptake) lower than average.

The typical timescale of full ENSO cycle is estimated to be about 48-52 months (Setoh et al 1999) whereas the timescale of the main meteorological parameters (global solar radiation (G), precipitation amount (P), air temperature (T)) is characterized by much higher month-to-month variability even after annual trend filtering. In order to filter the high-frequency oscillation in the time-series of atmospheric characteristics and monthly NEE, GPP, RE, ET anomalies the simple centered moving average smoothing procedure was applied. The moving averages (MA) of variables were calculated over 7 months (centered value ±3 months).

Statistical analysis included both simple correlation and cross-correlation analysis (Chatfield, 2004). Cross-correlation analysis was used to take into account the possible forward and backward time shifts of maximal anomalies of meteorological parameters and CO_2 and H_2O fluxes in respect to time of the ENSO culmination. To describe the relationships between atmospheric fluxes and meteorological parameters the monthly non-smoothed values were used.

3. Results

During the measuring period, two El Niño (August 2004 - March 2005 and October 2006 - January 2007) and one La Niña (November 2007 - April 2008) phenomena were observed. All events had moderate intensity. Both warm events could be classified as the Central Pacific or Modoki type, according to Ashok et al. (2007), since the SST-anomalies were centred in Nino3.4 and Nino4 regions (Figure 1).

Analysis of the intra-annual pattern of CO_2 and H_2O fluxes shows a relatively weak seasonal variability (Figure 2). The maximal values of GPP were obtained during the second part of the drier season - from August to October (278±13 gC m^{-2} $month^{-1}$) - which is also characterised by maximal values of incoming solar radiation. The mean monthly air temperature in the period varied from minimal values in August (19.2±0.2 °C) to maximal values in October (19.8±0.2 °C). The minimal GPP values were obtained in transition periods between more wet and dry seasons - in May - June and November - December (240±15 and 249±21 gC m^{-2} $month^{-1}$, respectively). These periods are also characterised by minimal amounts of incoming solar radiation (512±40 MJ m^{-2} $month^{-1}$). Maximal RE (206±10 gC m^{-2} $month^{-1}$) and values were obtained in October, which corresponds to the period of maximal air temperature and insolation. The local maximum of RE in April - May (199±4 gC m^{-2} $month^{-1}$) is also well correlated with a small increase of the air temperature in these months. The minimal RE was observed in February and June-August (174±10 and 187±15 gC m^{-2} $month^{-1}$, respectively). The intra-annual pattern of ET was closely related to the seasonal variability of GPP. The maximum values of ET were also observed in October (136±4 mm), in the month of maximal incoming solar radiation and highest values of air temperature. In spite of a large amount of precipitation and a high air temperature during the period from March to June, ET in this period was much lower than in September and October (e.g. 105±8 mm in April).

Comparisons of monthly NEE, GPP, RE, ET and SST-anomalies in Nino4 and Nino3.4 regions (Nino4 and Nino3.4 indexes) indicate relatively low correlations. Changes of the Nino4 index can explain about 12% of the observed variability in GPP (coefficient of determination, $r^2=0.12$ under significance level $p<0.05$), 9% of RE ($r^2=0.09$, $p<0.05$), 9% of NEE ($r^2=0.09$, $p>0.05$), 6% of ET ($r^2=0.06$, $p<0.05$) and only about 1% of transpiration (TR) ($r^2=0.01$, $p>0.05$). Similar values were obtained in correlation analysis for the Nino3.4 index. In the period of El Niño peak phases (September 2004 - January 2005 and October 2006 - January 2007) the values ET and GPP tend to increase in the study area. An increase of RE was indicated only during the second El Niño event from October 2006 to January 2007. The effect of El Niño on NEE was insignificant. The effect of La Niña on CO_2 and H_2O flux components was very small and manifested only in a slight increase of NEE.

Analysis of the temporal variability of the centered moving average values of ΔGPP (ΔGPP_{MA}) (Figure 3) in contrast to comparisons of absolute monthly GPP indicates a relatively high correlation between ΔGPP_{MA} and both Nino4 ($r^2=0.52$, $p<0.05$) and Nino3.4 ($r^2=0.60$, $p<0.05$) indexes. Close correlation between the intensity of ENSO events and ΔGPP_{MA} can be explained by the influence of ENSO initiating processes and ENSO itself on total cloud amount in the region and, as a result, on monthly sums of incoming G (Figure 4). Variability of G (ΔG_{MA}) is very closely correlated with Nino4 and Nino3.4 indexes ($r^2=0.48$, $p<0.05$ for both indexes) (Figure 4) and it can explain 69% of variability of GPP (r^2=0.69, p<0.05). The maximal deviations of ΔGPP_{MA} and ΔG_{MA} from mean values (averaged for the entire measuring period) are occurring 2-3 months before the peak phase of the ENSO events (Figure 5). The maximal cross-correlation coefficients in this period reached 0.76 for ΔG_{MA}, and 0.86 - for ΔGPP_{MA}. The effect of T changes (ΔT) on ΔGPP is very low (r^2=0.01, p>0.05).

The correlation between ΔT_{MA} and Nino4, Nino3.4 indexes are relatively low (r^2=0.15, p>0.05 for Nino4 and r^2=0.05, p>0.05 for Nino3.4) and it can explain the very weak correlations between ΔRE_{MA} and ENSO indexes (r^2=0.10, p<0.05 for Nino4 and r^2=0.04, p>0.05 for Nino3.4) (Figures 3-4). The maximal deviations of T_{MA} and RE_{MA} from mean values (averaged for the entire measuring period) are occurring 2 months after the peak phase of the ENSO events and it has negative sign (Figure 5). The cross-correlation coefficient in this period is -0.53 (p<0.05).

Despite the relatively close dependence of ΔGPP_{MA} on ENSO intensity, the correlations between ΔNEE_{MA} and Nino4, Nino3.4 indexes are lower (r^2 = 0.31, p<0.05 for Nino4 and r^2 = 0.37, p<0.05 for Nino3.4), mainly because of their very low correlation during the first part of the measuring period (before December 2005). During the second part of the considered period (from June 2006 to June 2008) with one strong El Niño (October 2006 - January 2007) and one La Niña (November 2004 - April 2008) events ΔNEE_{MA} and Nino4, Nino3.4 indexes are correlated much better. It can be explained by the influence of ΔRE_{MA} on ΔNEE_{MA} dynamics that is mainly governed by temperature variability and which is, as already mentioned, very poorly correlated with Nino4/Nino3.4 indexes (Figures 3-4).

Taking into account that the monthly anomalies of NEE might be biased by a still unaccounted advection effects at night-time, despite u_* filtering, , we additionally examined NEE at midday (10:00-14:00), when turbulent mixing is typically well developed. Data analysis based on midday NEE shows a similar clear relationship with the ENSO index (Figure 6) with r^2 = 0.59 under p<0.05. The maximal deviations of both NEE_{MA} and midday NEE_{MA} from the their mean values occurred simultaneously within the peak phase of the ENSO events (Figure 5).

Analysis of the temporal variability of the moving average values of monthly ET (ΔET_{MA}) showed a high correlation to ENSO activity as well: r^2 = 0.72, p<0.05 for Nino4 and r^2 = 0.70, p<0.05 for Nino3.4 (Figure 7), probably also triggered by G_{MA}, which in turn correlated strongly with both the Nino4 and the Nino3.4 index. Periods of extreme ΔET_{MA} values and maximal ENSO intensity occurred simultaneously (Figure 5). Correlations between ΔET and ΔT, as well as between ΔET and ΔP, are insignificant - r^2=0.09 (p>0.05) and r^2=0.01 (p>0.05), respectively. However, figures 4 and 5 clearly show a time delay in ΔP_{MA} oscillation, relative to Nino4 and Nino3.4 patterns. The maximal negative deviations of ΔP_{MA} are observed about eight months before,(cross-correlation between ΔP_{MA} and Nino 4 index 0.72, p<0.05) and maximal positive deviation of ΔP_{MA}

- about four-five months after the peak phases of ENSO (cross-correlation between ΔP_{MA} and Nino 4 index - 0.40, $p<0.05$), respectively.

To explain a very low sensitivity of ET to P changes, we analysed the intra-annual variability of the ratio between ET and potential evaporation (PET), as well as between ET and P. PET was derived using the well-known Priestley and Taylor (1972) approach and it is equal to evaporation from wet ground or open water surface.

The mean annual ET during the measuring period is considerably lower than P (ET/P=0.742). Over the annual course, the ratio varied between 0.58 (in March and November) to 1.85 (in August and October). During dry periods before the positive phase of ENSO, the mean values of the ET/P ratio grow up to 1.9-2.1. During the periods of negative Nino4 and Nino3.4 anomalies the mean monthly ET/P ratio fell, in some months, down to 0.3. Correlation analysis of temporal variability of $\Delta(ET/P)$ and $\Delta(ET/P)_{MA}$ ratios and Nino4 and Nino3.4 indexes (Figure 7) did not show any statistically significant relationships. However, it should be mentioned that the temporal pattern of $\Delta(ET/P)$ and $\Delta(ET/P)_{MA}$ is characterised by two peaks that were observed in July of 2005 and April 2007, about 6-8 months prior to the El Niño culmination (Figure 7).

The monthly mean ET/PET ratio has a feeble intra-annual course with maximum in June (0.93±0.03) and with minima in February and October (0.84±0.06). The averaged annual ET/PET ratio for the entire measuring period was 0.880±0.055. The minimal values of $(ET/PET)_{MA}$ ($(ET/PET)_{MA}$=0.81) were observed during the El Niño culmination in 2005-2006, and the maximal values, during the period of maximal intensity of La Niña in 2008 ($(ET/PET)_{MA}$=0.93). Thus, monthly ET rates are relatively close to PET values during the whole year including the periods of maximal ENSO activity. The relative soil water content of the upper 30 cm horizon calculated using the Mixfor-SVAT model during the entire period of the field measurements, including the periods with maximal values of the ET/P ratio, was always higher than 80%. This, together with the ET/PET ratio, is a clear indicator of permanently sufficient soil moisture conditions in the study area, including periods of El Niño and La Niña culminations, explaining the very low sensitivity of ΔET to ΔP.

4. Discussion

The provided analysis of the temporal variability for the main components of carbon and water balances in the tropical rainforest showed a high correlation between Nino4 and Nino3.4 SST anomalies, characterising the ENSO intensity with GPP_{MA} and ET_{MA} deviations from monthly averages over the entire measuring period. Application of the centered moving average smoothing procedure allows us to filter the high-frequency month-to-month oscillations in the time-series of atmospheric characteristics caused by local and regional circulation processes that are not directly connected with ENSO activity. The relationships between ΔGPP_{MA}, ΔET_{MA} and Nino4 and Nino3.4 indexes are mainly governed on the one hand by the dependency of the incoming solar radiation on ENSO development – surface water warming in Nino 3.4 and 4 regions generally results in a decrease of cloudiness above the study region and thus – in increase of incoming solar radiation. On the other hand there are many data about a high correlation between monthly GPP and ET rates and incoming and absorbed solar radiation (e.g. Ibrom et al., 2008). The effects of monthly air temperature and precipitation changes on ΔGPP and ΔET variability are relatively poor, mainly due to the low correlations between ΔT_{MA}, ΔP_{MA} and ENSO intensity.

The cross-correlation analysis (Fig. 5) shows that the ΔGPP_{MA} and ΔG_{MA} have a small 2-3 month backward shift relatively to the course of Nino4 SST, i.e. the maxima in GPP_{MA} occur earlier than ENSO culmination in the central Pacific (Nino4 SST anomaly). The maximal values of ΔE_{MA} occurred simultaneously with El Niño and La Niña culminations. Such an effect of El Niño episodes on G can be explained, as mentioned above, by a decrease of the cloud amount in the region of Indonesia, due to the El Niño-associated shift of the Walker circulation cell, and corresponding zone of deep convection, from the maritime continent of Indonesia toward the dateline following SST anomalies displacement. El Nino usually begins in April, and toward August-September the ascending branch of the Walker cell leaves Indonesia and migrates eastward to the Pacific. Therefore, 3-4 months before the El Niño culmination in December-January, a decrease in cloud amount is observed over Indonesia. Weakening of El Niño, in turn, leads to a backward shift of intensive convection zone westward. It can result in increasing precipitation amounts in the region during the second half of the wet period after passing the maximal El Niño activity and also the gradual increase of the cloudiness and decrease of incoming solar radiation. The opposite effect takes place during the La Niña with similar phase shift: simultaneously, with the spreading of a negative SST anomaly over the Pacific, the increasing of deep convection over Indonesia occurs, which results in an increase of cloudiness and precipitation, being more pronounced as it falls into the dry period of the year. The lower panels of Figure 4 indicate however, that the decrease of radiation due to increase of cloudiness does not depend linearly on La Nina intensity, reaching a saturation state at approximately -20..-30 MJ m^{-2} $month^{-1}$.

A relatively poor correlation between ΔT_{MA} patterns and ENSO activity and an insignificant influence of ΔT on ΔGPP and ΔET can be mainly explained by the small intra-annual amplitude of the air temperature in the study area not exceeding 1.0 °C, as well as by the low dependence of the air temperature on incoming solar radiation. The mean monthly temperatures ranged in the intra-annual course between 19.5 °C and 20.5 °C. Maximal air temperatures do not exceed 28.5 °C, even on sunny days. Such optimal thermal conditions with high precipitation amount provide sufficient soil moistening and relatively comfortable conditions for tree growth during the whole year. As is was already mentioned even during the El Niño culmination in 2005-2006 the ET/PET did not decrease below 0.74, $(ET/PET)_{MA}$>0.81, and the relative soil water content of the upper 30 cm horizon was always higher than 80%.

The analysis of absolute and relative changes of GPP and ET during the periods of maximal El Niño and La Niña activities showed that GPP during the El Niño culminations of 2005 and 2007 increased by about 20 gC m^{-2} $month^{-1}$ (6-7%). ΔGPP_{MA} was about 9 gC m^{-2} $month^{-1}$ (2-3%), ΔET - about 40 mm $month^{-1}$ (about 30%) and ΔET_{MA} - about 10 mm $month^{-1}$ (6-7%). Thus, the maximal ΔGPP was two times lower than the mean annual amplitude of GPP (Figure 2). The maximal ΔET was equal to the annual amplitude of ET (Figure 2). During the La Niña culmination of 2008 the maximal relative changes of GPP were higher than the relative changes observed during El Niño events: ΔGPP was about -22 gC m^{-2} $month^{-1}$ (8%), ΔGPP_{MA} - about -12 gC m^{-2} $month^{-1}$ (4%). The maximal decrease of ΔET in the period was relatively small: ΔET - about -12 mm $month^{-1}$ (10%) and ΔET_{MA} - about -5 mm $month^{-1}$ (4%). ΔET was about 3 times lower than the mean annual amplitude of ET. Interestingly the radiation dependent GPP (as represented by smoothed 7 month mean) does not demonstrate any prolonged constant period during La Nina phases though the radiation does. During the first cold event the GPP-reduction is not as strong as during the second one, although the G-reductions are nearly of same strength. It could be assumed that in the first case the effect of radiation decrease on GPP was compensated by other factors like slight increase of the air temperature.

Additionally, we investigated the influence of other climatic anomalies in the region on CO_2 and H_2O fluxes of the tropical rainforest, such as the Madden–Julian oscillation (MJO) and the Indian Ocean Dipole (IOD). The MJO is characterised by an eastward propagation of large regions of enhanced and suppressed deep convection from the Indian ocean toward central Pacific (Zhang, 2005). Each MJO cycle lasts approximately 30–60 days and includes wetter (positive) and drier (negative) phases. As an estimation of deep convection intensity in the tropics, the outgoing long-wave radiation (OLR) measured at the top of the atmosphere is commonly used. It was recently shown that 6-12 months prior to the onset of an El Niño episode a drastic intensification of the MJO occurs in the Western Pacific (Zhang and Gottschalck, 2002; Lau, 2005; Hendon et al., 2007; Gushchina and Dewitte, 2011). Furthermore, MJO behaviour varies significantly during the ENSO cycle: it is significantly decreased during the maxima of conventional El Niño episodes, while it is still active during the peak phase of central Pacific events. MJO rarely occurs during La Niña episodes (Gushchina and Dewitte, 2012). As MJO is strongly responsible for intra-seasonal variation of precipitation in the study region, the occurrence of MJO events was compared to the significant anomalies of ET/P ratio and of key meteorological variables. No evidence of MJO influence is observed: the positive and negative anomalies of ET/P ratio are associated to positive, negative and zero anomalies of OLR, filtered in the MJO interval. Also, no significant relation emerged from the correlation analysis.

Correlations between MJO index (Wheeler and Kiladis, 1999; Gushchina and Dewitte, 2011), and the deviations of key meteorological parameters from monthly averages during the study period were very low: $r^2 = 0.03$ for T, $r^2 = 0.03$ for P and $r^2 = 0.01$ for G ($p>0.05$, in both cases).

The Indian Ocean Dipole (IOD) is characterised by changes of the SST in the western Indian Ocean, resulting in intensive rainfall in the western part of Indonesia during the positive phase and corresponding precipitation reduction during the negative phase (Saji et al., 1999). To find a possible influence of IOD events on temporal variability of meteorological parameters and CO_2 and H_2O fluxes, the monthly mean IOD index (Dipole Mode Index, DMI) was used. Results showed that with respect to the western part of Indonesia situated close to Indian Ocean the IOD phenomenon has no significant impact on meteorological conditions and fluxes of the area of Central Sulawesi.

5. Conclusions

CO_2 and H_2O fluxes in the mountainous tropical rainforest in Central Sulawesi in Indonesia showed a high sensitivity of monthly GPP and ET to ENSO intensity for the period from January 2004 to June 2008. This was mainly governed by the high dependency of incoming solar radiation (*G*) to Nino4 and Nino3.4 SST changes and the strong sensitivity of GPP and ET on *G*.

Interestingly, we observed time shifts between the SST anomalies and smoothed GPP anomalies driven by radiation anomalies. The maximal deviations of GPP and G from their mean values occurred 2-3 months before the peak phase of the ENSO events. The effect of ENSO intensity on RE was relatively low, mainly due to its weak effect on air temperature. Anyway, the small cross-correlation between RE and ENSO intensity had a compensatory effect on the timing of NEE, which thus was - like evapotranspiration - in synchrony with El Niño culminations. Unlike the observations in other tropical sites, precipitation variations had no influence on the CO_2 and H_2O fluxes at study site, mainly due to the permanently sufficient soil moisture condition in the study area.

Other climatic anomalies in the Western Pacific region, such as the Indian Ocean Dipole and the Madden–Julian oscillation, did not show any significant effect on neither the meteorological conditions nor the CO_2 and H_2O fluxes in the investigated mountainous tropical rainforest in Central Sulawesi.

It is important to emphasise that the considered observation period does not cover a period with extreme El Niño events, such as, e.g., the 1982-83 and 1997-98 events, when the anomaly of Nino3.4 SST, during several months, exceeded 2.6°C and more significant changes of surface water availability were observed. Also, in lowland parts of Sulawesi, characterised by higher temperatures and lower precipitation, the vegetation response to ENSO events is likely to be different and more pronounced (Erasmi et al., 2009).

All observed ENSO events during the selected period are classified as Central Pacific type. Recently, Yeh et al. (2009) showed that under projected climate change the proportion of Central Pacific ENSO events might increase. Furthermore, Cai et al. (2014, 2015) showed that current projections of climate change for the 21st century suggest an increased future likelihood of both El Niño and La Niña events. Based on the results of our study, potential increases in ENSO activity would results in an increased variability of the CO_2 and H_2O exchange between atmosphere and the tropical rainforests in such regions.

Acknowledgement

The study was supported by the German Science Foundation under the projects "Stability of Rainforest Margins in Indonesia", STORMA (SFB 552), "Ecological and Socioeconomic Functions of Tropical Lowland Rainforest Transformation Systems (Sumatra, Indonesia)" (SFB 990) and KN 582/8-1. The Russian Science Foundation (grant RSCF 14-27-00065) supports A. Olchev in part of the model development.

Reference

1. Aiba, S., and Kitayama, K.: Effects of the 1997-98 El Niño drought on rain forests of Mount Kinabalu, Borneo, Journal of Tropical Ecology, 18, 215–230, 2002
2. Ashok, K., Behera, S. K., Rao S. A., Weng H., Yamagata, T.: El Niño Modoki and its possible teleconnection. J. Geophys. Res. 112, C11007, doi:10.1029/2006JC003798, 2007
3. Ashok, K. and Yamagata, T.: The El Niño with a difference. Nature, 461, 481-484, 2009
4. Aubinet, M., A. Grelle, A. Ibrom, U. Rannik, J. Moncrieff, T. Foken, A. S. Kowalski, P. H. Martin, P. Berbigier, C. Bernhofer, R. Clement, J. Elbers, A. Granier, T. Grunwald, K. Morgenstern, K. Pilegaard, C. Rebmann, W. Snijders, Valentini R. and Vesala T.: Estimates of the annual net carbon and water exchange of forests: The EUROFLUX methodology. Advances In Ecological Research, 30, 113-175, 2000

5. Aubinet, M., Vesala, T., and Papale, D. (Eds.): Eddy Covariance: A Practical Guide to Measurement and Data Analysis. Springer Atmospheric Sciences, Springer Verlag, Dordrecht, The Netherlands, 438 pp., 2012
6. Burba, G.G., McDermitt, D.K., Grelle, A., Anderson, D.J., Xu, L.: Addressing the influence of instrument surface heat exchange on the measurements of CO_2 flux from open-path gas analyzers. Global Change Biology, 14, 1-23, 2012
7. Cai, W., Borlace, S., Lengaigne, M., van Rensch, P., Collins, M., Vecchi, G., Timmermann, A., Santoso, A., McPhaden, M.J., Wu, L., England, M.H., Wang, G., Guilyardi, E. and Jin, F.-F.: Increasing frequency of extreme El Niño events due to greenhouse warming. Nature Climate Change, 4, 111-116, 2014
8. Cai, W., Wang, G., Santoso, A., McPhaden, M., Wu, L., Jin, F-F., Timmermann, A., Collins, M., Vecchi, G., Lengaigne, M., England, M., Dommenget, D., Takahashi, K., Guilyardi, E.: More frequent extreme La Niña events under greenhouse warming. Nature Climate Change, 5, 132-137, 2015
9. Chatfield, C.: The Analysis of Time series, An Introduction, sixth edition. Chapman & Hall/CRC, New York, 333 pp., 2004
10. Chen, D. and Chen, H. W.: Using the Koppen classification to quantify climate variation and change: An example for 19012010. Environmental Development, 6, 69-79, 2013
11. Ciais, P., Piao, S.L., Cadule, P., Friedlingstein, P., and Chedin, A.: Variability and recent trends in the African terrestrial carbon balance.Biogeosciences, 6, 1935-1948, 2009
12. Clark, D.A., and Clark, D.B.: Climate-induced variation in canopy tree growth in a Costa Rican tropical rain forest. Journal of Ecology, 82, 865-872, 1994
13. Download Climate Timeseries: http://www.esrl.noaa.gov/psd/gcos_wgsp/Timeseries/, 24 April 2013
14. Erasmi, S., Propastin, P., Kappas, M., and Panferov, O.: Patterns of NDVI variation over Indonesia and its relationship to ENSO during the period 1982-2003, J Climate, 22(24), 6612–6623, 2009
15. Falge, E., Reth, S., Brüggemann, N., Butterbach-Bahl, K., Goldberg, V., Oltchev, A., Schaaf, S., Spindler, G., Stiller, B., Queck, R., Köstner, B., Bernhofer, C.: Comparison of surface energy exchange models with eddy flux data in forest and grassland ecosystems of Germany. J. Ecological Modelling, 188 (2-4), 174-216, 2005
16. Falk U., Ibrom A., Kreilein H., Oltchev A., and Gravenhorst, G.: Energy and water fluxes above a cacao agroforestry system in Central Sulawesi, Indonesia, indicate effects of land-use change on local climate Met. Zeitsch., 14(2), 219-225, 2005

17. FAO: Global forest resources assessment 2010: Main report, FAO Forestry Paper 163, Rome, Italy, 340 pp., 2010
18. Feely, R.A., Wanninkhof, R., Takahashi, T., and Tans, P.: Influence of El Niño on the equatorial Pacific contribution to atmospheric CO_2 accumulation. Nature 398, 597-601, 1999
19. Fisher, J.B., Sikka, M., Sitch, S., Ciais, P., Poulter, B., Galbraith, D., Lee, J.-E., Huntingford, C., Viovy, N., Zeng, N., Ahlstrom, A., Lomas, M.R., Levy, P.E., Frankenberg, C., Saatchi, S., and Malhi, Y.: African tropical rainforest net carbon dioxide fluxes in the twentieth century. Phil Trans R Soc B, 368, 20120376, http://dx.doi.org/10.1098/rstb.2012.0376, 2013
20. Gerold, G., Leemhuis, C.: Effects of “ENSO-events” and rainforest conversion on river discharge in Central Sulawesi (Indonesia). In: Tropical Rainforests and Agroforests under Global Change Environmental Science and Engineering, T. Tscharntke, Ch. Leuschner, E. Veldkamp, H. Faust, E. Guhardja, A. Bidin (Eds), 327-350, 2010
21. Grace, J., Lloyd, J., McIntyre, J., Miranda, A., Meir, P., Miranda, H., Nobre, C., Moncrieff, J.B., Massheder, J.M., Malhi, Y., Wright, I., and Gash, J.C.: Carbon dioxide uptake by an undisturbed tropical rain forest in south-west Amazonia, 1992 to 1993. Science, 270, 778-780, 1995
22. Grace, J., Malhi, Y., Lloyd, J., McIntyre, J., Miranda, A.C., Meir, P., and Miranda, H.S.: The use of eddy covariance to infer the net carbon uptake of Brazilian rain forest. Global Change Biology, 2, 209-218, 1996
23. Graf, H.-F., and Zanchettin, D.: Central Pacific El Niño, the “subtropical bridge,”and Eurasian climate, J. Geophys. Res., 117, D01102, doi:10.1029/2011JD016493, 2012
24. Gushchina, D., and Dewitte, B.: The relationship between intraseasonal tropical variability and ENSO and its modulation at seasonal to decadal timescales, Cent. Eur. J. Geosci., 1(2), 175-196, 2011, DOI: 10.2478/s13533-011-0017-3
25. Gushchina, D., and Dewitte, B.: Intraseasonal tropical atmospheric variability associated to the two flavors of El Niño. Month. Wea. Rev., 140, (11). 3669-3681, 2012
26. Hansen, M.C., Potapov, P. V., Moore, R., Hancher, M., Turubanova, S.A., Tyukavina, A., Thau, D., Stehman, S.V., Goetz, S.J., Loveland, T.R., Komardeey, A. Egorov, A., Chini, L., Justice, C.O., and Townshend, J.R.G.. High-Resolution Global Maps of 21st-Century Forest Cover Change. Science, 342, 850-853, 2013
27. Hirano, T., Segah, H., Harada, T., Limin, S., June, T., Hirata, R., and Osaki, M.: Carbon dioxide balance of a tropical peat swamp forest in Kalimantan, Indonesia. Global Change Biology, 13, 412–425. doi: 10.1111/j.1365-2486.2006.01301.x, 2007
28. Ibrom, A., Olchev, A., June, T., Ross, T., Kreilein, H., Falk, U., Merklein, J., Twele, A., Rakkibu, G., Grote, S., Rauf, A., and Gravenhorst, G.: Effects of land-use change on matter and

energy exchange between ecosystems in the rain forest margin and the atmosphere. In The stability of tropical rainforest margins: Linking ecological, economic and social constraints. Eds. T. Tscharntke, C. Leuschner, M. Zeller, E. Guhardja and A. Bidin, Springer Verlag, Berlin, pp. 463 – 492, 2007

29. Ibrom, A., Oltchev, A., June, T., Kreilein, H., Rakkibu, G., Ross, Th., Panferov, O., Gravenhorst, G.: Variation in photosynthetic light-use efficiency in a mountainous tropical rain forest in Indonesia. Tree Physiology, 28(4), 499–508, 2008

30. Järvi, L., Mammarella, I., Eugster, W., Ibrom, A., Siivola, E., Dellwik, E., Keronen, P., Burba, G., Vesala, T.: Comparison of net CO_2 fluxes measured with open- and closed-path infrared gas analyzers in urban complex environment. Boreal Environmental Research, 14, 499–514, 2009

31. Kug, J.-S., Jin, F.-F., and An, S.-I.: Two types of El Niño events: Cold tongue El Niño and warm pool El Niño, J. Climate, 22, 1499–1515, 2009

32. Larkin, N. K., and Harrison, D.E.: Global seasonal temperature and precipitation anomalies during El Niño autumn and winter. Geophysical Research Letters, 32, L13705, 2005, doi:10.1029/2005GL022738.

33. Lau, W. K. M.: El Niño Southern Oscillation connection. Intraseasonal Variability of the Atmosphere-Ocean Climate System, W. K. M. Lau, and D. E. Waliser., Eds., Praxis Publishing, Chichester, UK, 271-300, 2005

34. Lewis, S.L., Lopez-Gonzalez, G., Sonke, B., Affum-Baffoe, K., Baker, T.R., Ojo, L.O., Phillips, O.L., Reitsma, J.M., White, L., Comiskey, J.A., Djuikouo, K. M.-N., Ewango, C.E.N., Feldpausch, T.R., Hamilton, A.C., Gloor, M., Hart, T., Hladik, A., Lloyd, J., Lovett, J.C., Makana, J.-R., Malhi, Y., Mbago, F.M., Ndangalasi, H.J., Peacock, J., Peh, K. S.-H., Sheil, D., Sunderland, T., Swaine, M.D., Taplin, J., Taylor, D., Thomas, S.C., Votere, R. and Woll, H.: Increasing carbon storage in intact African tropical forests. Nature, 457: 1003-1006, 2009

35. Malhi, Y., Baldocchi, D.D., and Jarvis, P.G.: The carbon balance of tropical, temperate and boreal forests. Plant Cell and Environment, 22, 715-740, 1999

36. Malhi, Y.: The carbon balance of tropical forest regions, 1990–2005, Current Opinion in Environmental Sustainability, 2(4), 237–244, 2010

37. Moser, G., Schuldt, B., Hertel, D., Horna, V., Coners, H., Barus, H., and Leuschner, C.: Replicated throughfall exclusion experiment in an Indonesian perhumid rainforest: wood production, litter fall and fine root growth under simulated drought. Global Change Biology, 20, 1481–1497, doi: 10.1111/gcb.12424, 2014

38. Oltchev, A., Cermak, J., Nadezhdina, N., Tatarinov, F., Tishenko, A., Ibrom, A., Gravenhorst, G.: Transpiration of a mixed forest stand: field measurements and simulation using SVAT models. J. Boreal Environmental Reserach, 7(4), 389-397, 2002

39. Olchev, A., Ibrom, A., Ross, T., Falk, U., Rakkibu, G., Radler, K., Grote, S., Kreilein, H., and Gravenhorst G.: A modelling approach for simulation of water and carbon dioxide exchange between multi-species tropical rain forest and the atmosphere. J. Ecological Modelling, 212, 122–130, 2008
40. Panferov, O., Ibrom, I., Kreilein, H., Oltchev, A., Rauf, A., June, T., Gravenhorst, G. and Knohl, A.: Between deforestation and climate impact: the Bariri Flux tower site in the primary montane rainforest of Central Sulawesi, Indonesia. The Newsletter of FLUXNET 2(3), 17-19, 2009
41. Phillips, O.L., Aragao, L., Lewis, S.L., Fisher, J.B., Lloyd, J., Lopez-Gonzalez, G., Malhi, Y., Monteagudo, A., Peacock, J., Quesada, C.A., van der Heijden, G., Almeida, S., Amaral, I., Arroyo, L., Aymard, G., Baker, T.R., Banki, O., Blanc, L., Bonal, D., Brando, P., Chave, J., de Oliveira, A.C.A., Cardozo, N.D., Czimczik, C.I, Feldpausch, T.R., Freitas, M.A., Gloor, E., Higuchi, N., Jimenez, E., Lloyd, G., Meir, P., Mendoza, C., Morel, A., Neill, D.A., Nepstad, D., Patino, S., Penuela, M.C., Prieto, A., Ramirez, F., Schwarz, M., Silva, J., Silveira, M., Thomas, A.S., ter Steege, H., Stropp, J., Vasquez, R., Zelazowski, P., Davila, E.A., Andelman, S., Andrade, A., Chao, K.-J., Erwin, T., Di Fiore, A., Honorio, C. E., Keeling, H., Killeen, T.J., Laurance, W.F., Cruz, A.P., Pitman, N.C.A., Vargas, P.N., Ramirez-Angulo, H., Rudas, A., Salamao, R., Silva, N., Terborgh, J. and Torres-Lezama, A.: Drought sensitivity of the Amazon rainforest. Science 323, 1344-1347, 2009
42. Setoh, T., Imawaki, S., Ostrovskii, A. and Umatani S.: Interdecadal Variations of ENSO Signals and Annual Cycles Revealed by Wavelet Analysis. Journal of Oceanography, 55, 385-394, 1999
43. Priestley, C.H.B., and Taylor, R.J.: On the assessment of surface heat flux and evaporation using large-scale parameters. Monthly Weather Review, 100 (2), 81-92, 1972
44. Rasmusson, E.M., and Carpenter, T.H.: Variations in tropical sea surface temperature and surface wind fialds associated with the Southern Oscillation/ El Niño. Monthly Weather Review, 110, 354-384, 1982
45. Rayner, P. J., and Law, R. M.: The relationship between tropical CO2 fluxes and the El Niño-Southern Oscillation, Geophys. Res. Lett., 26(4), 493–496, doi:10.1029/1999GL900008, 1999
46. Reichstein, M., Bahn, M., Ciais, P., Frank, D., Mahecha, M.D., Seneviratne, S.I., Zscheischler, J., Beer, C., Buchmann, N., Frank, D.C., Papale, D., Rammig, A., Smith, P., Thonicke, K., van der Velde, M., Vicca, S., Walz, A., Wattenbach, M.: Climate extremes and the carbon cycle. Nature, 500, 287- 295, 2013
47. Reverter, B.R., Carrara, A., Fernández, A., Gimeno, C., Sanz, M.J., Serrano-Ortiz, P., Sánchez-Cañete, E.P., Were, A., Domingo, F., Resco, V., Burba, G.G., Kowalski, A.S.: Adjustment of

annual NEE and ET for the open-path IRGA self-heating correction: Magnitude and approximation over a range of climate. Agricultural and Forest Meteorology, 151(12), 1856-1861, 2011

48. Saji, N. H., Goswami, B. N., Vinayachandran, P. N., Yamagata, T.: A dipole mode in the tropical Indian Ocean. Nature, 401, 360-363, 1999
49. Wang, C.: Atmospheric circulation cells associated with the El Niño-Southern Oscillation. J. Climate, 15, 399-419, 2002
50. Wheeler, M. C., and Kiladis, G. N.: Convectively coupled equatorial waves: Analysis of clouds and temperature in the wavenumber–frequency domain. J. Atmos. Sci., 56, 374–399, 1999.
51. Yeh, S.-W., Kug, J.-S., Dewitte, B., Kwon, M.-H., Kirtman, B., and Jin, F.-F.: El Niño in a changing climate. Nature, 461, 511-514, 2009
52. Zhang, C.: Madden-Julian Oscillation. Reviews of Geophysics, 43, RG2003, 2005, doi: 10.1029/2004RG000158.
53. Zhang, C., and Gottschalck, J.: SST Anomalies of ENSO and the Madden–Julian oscillation in the equatorial Pacific. J. Climate, 15, 2429–2445, 2002

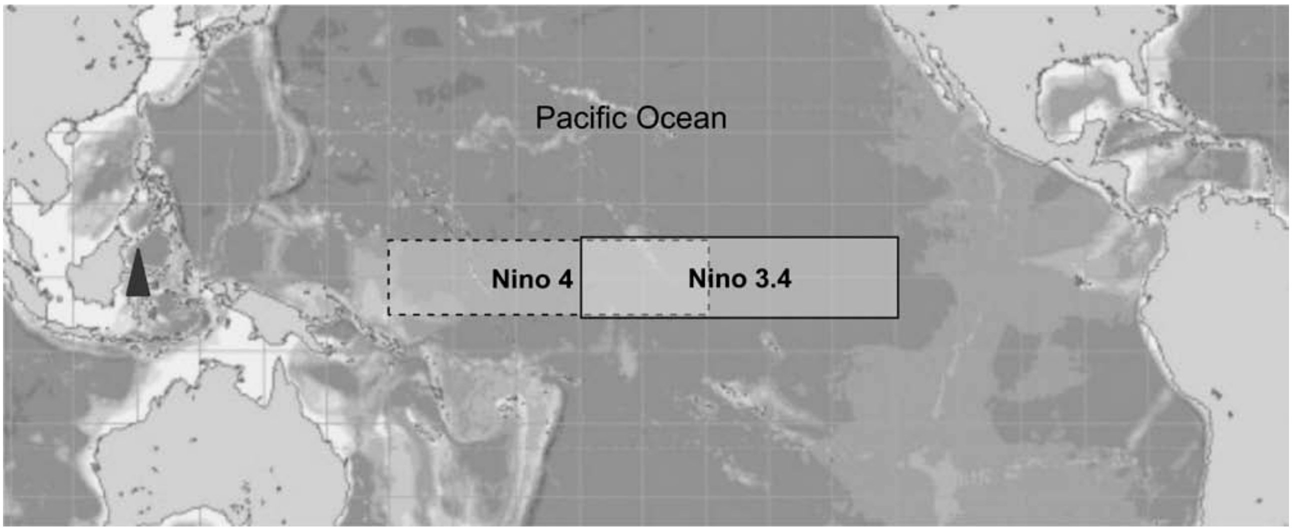

Figure 1. Geographical location of a study area (marked by black triangle) in tropical rain forest in Central Sulawesi (Indonesia) and Nino4 and Nino3.4 regions.

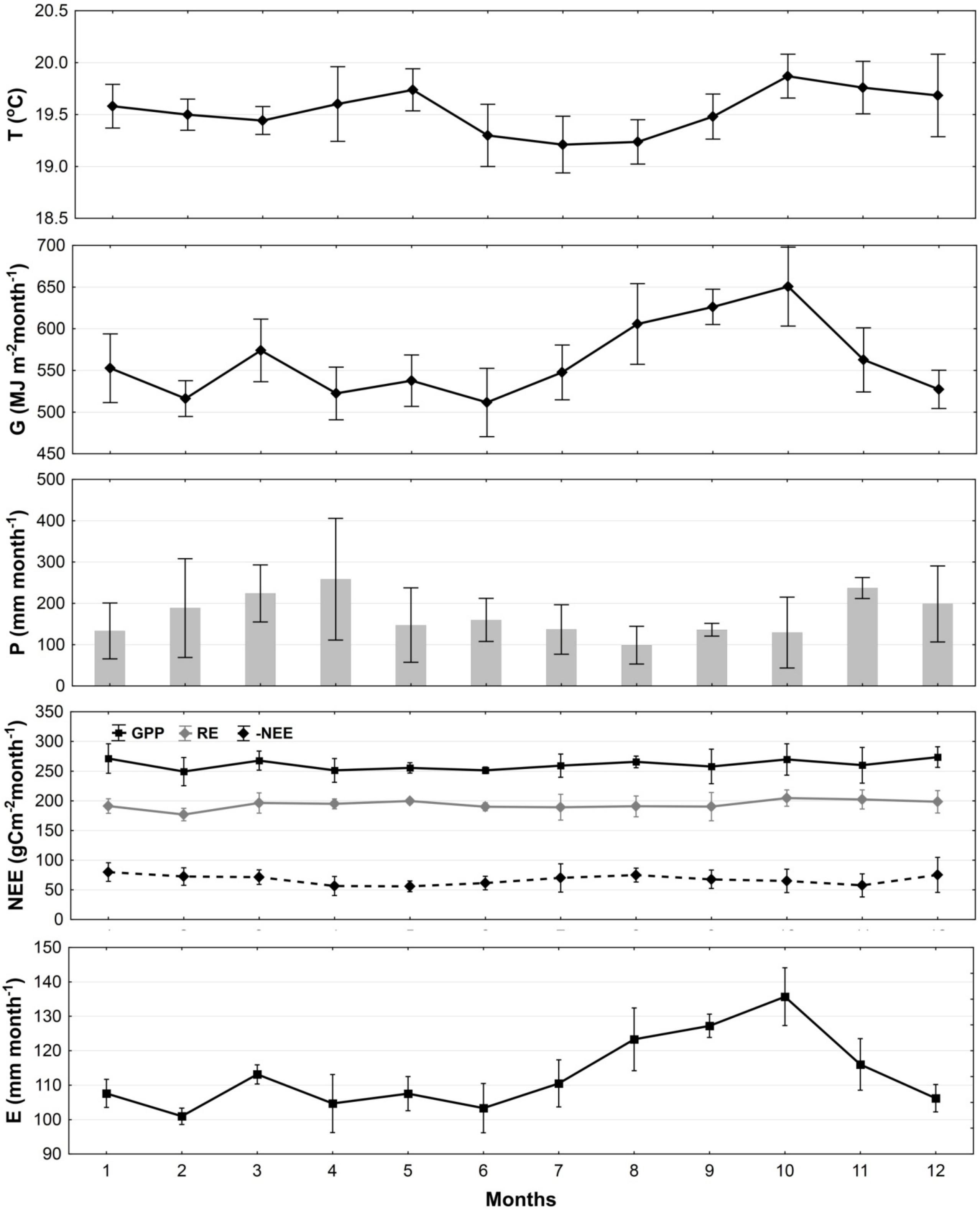

Figure 2. Mean intra-annual courses of air temperature (T), global solar radiation (G), precipitation (P), NEE, GPP, RE and ET for the tropical rain forest in Bariri. Vertical whiskers indicate standard deviations (SD).

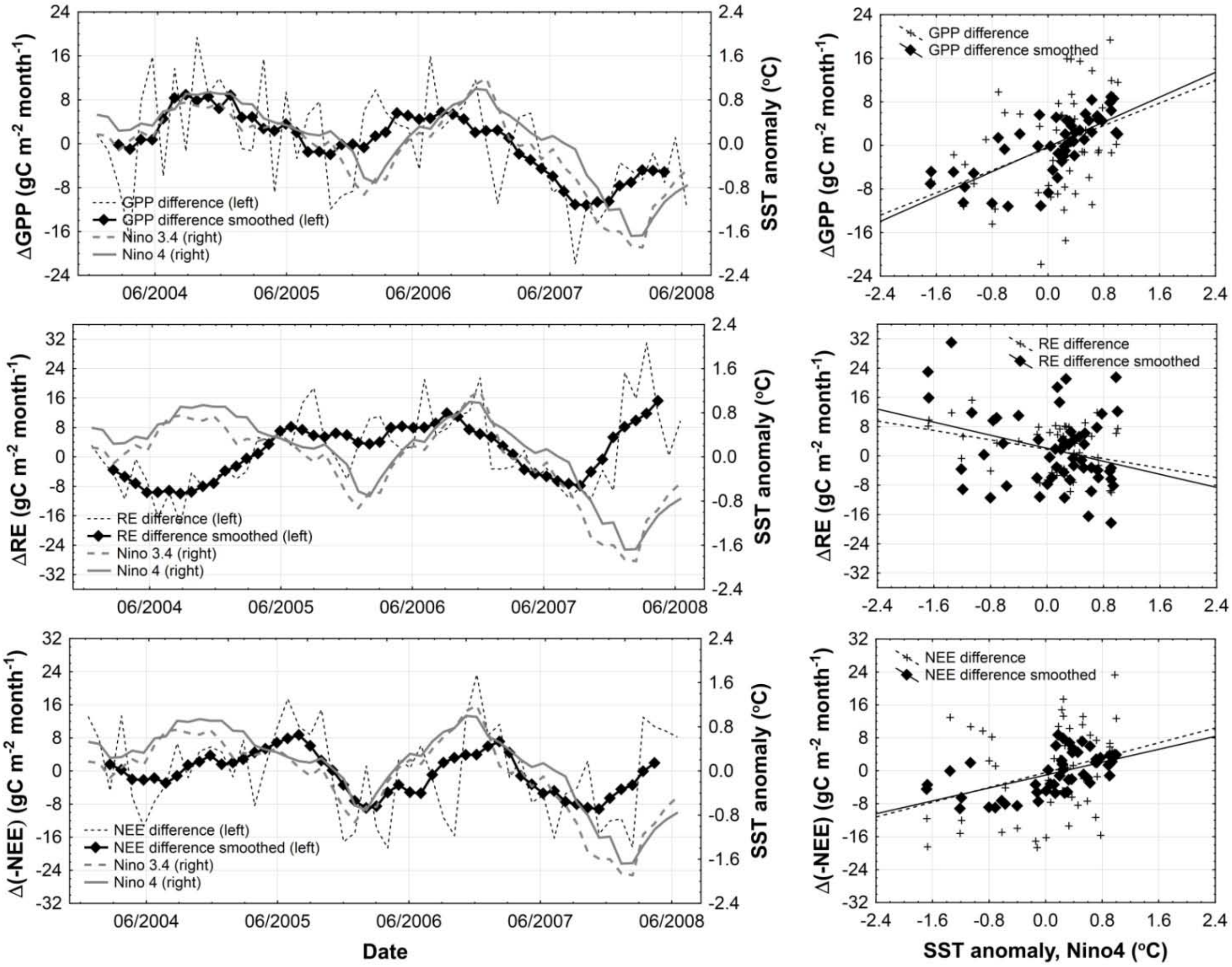

Figure 3. Comparisons of inter-annual pattern of SST anomalies in Nino4 and Nino3.4 zones of equatorial Pacific with variability of both deviations and 7 month (±3 months) moving average deviations of monthly GPP, RE and NEE values from mean monthly values of GPP, RE and NEE averaged over the entire measuring period from 2004 to 2008.

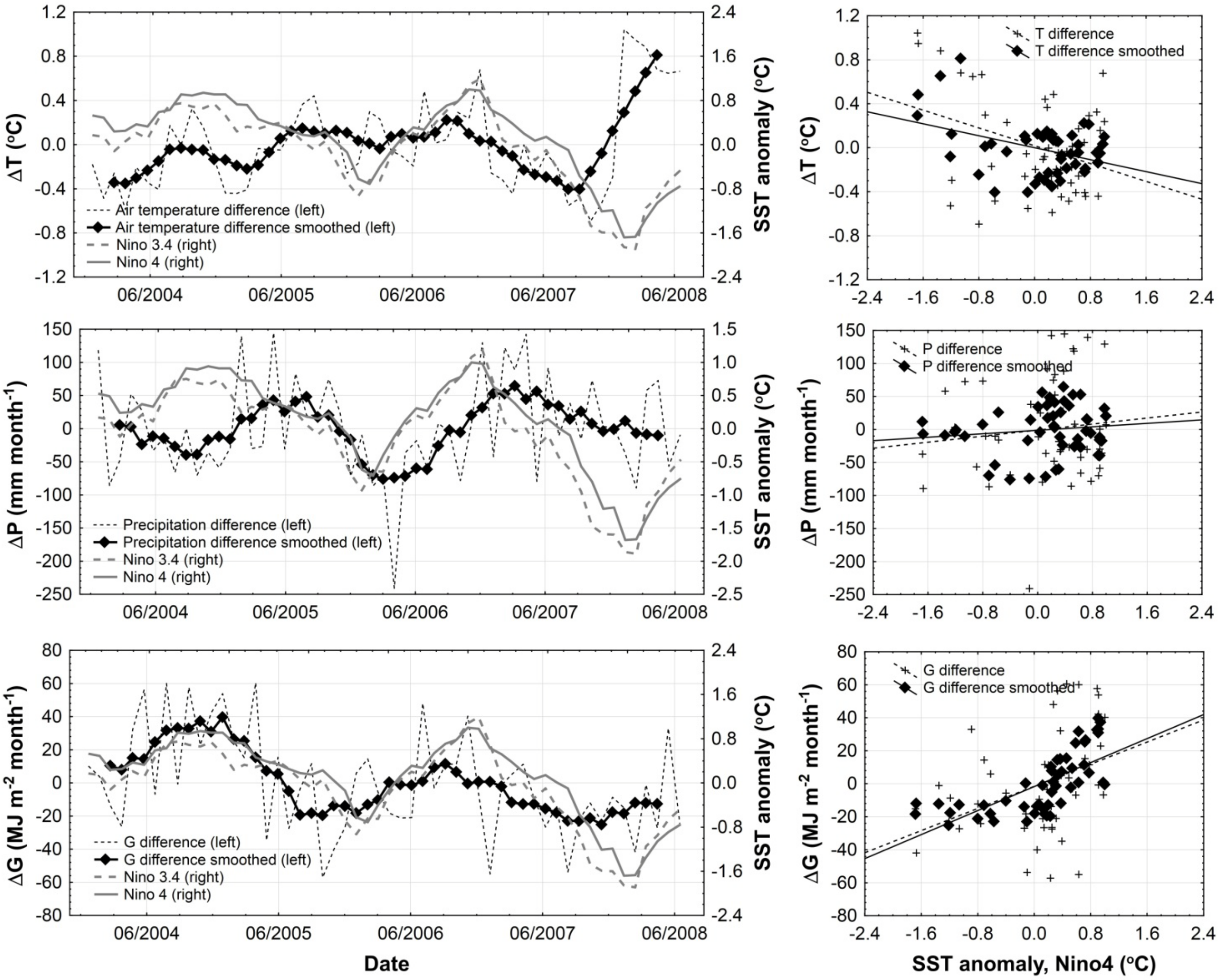

Figure 4. Comparisons of inter-annual pattern of SST anomalies in Nino4 and Nino3.4 zones of equatorial Pacific with variability of both deviations and 7 month (±3 months) moving average deviations of monthly air temperature (T), precipitation (P) and global radiation (G) values from mean monthly values of T, P and G averaged over the entire measuring period from 2004 to 2008.

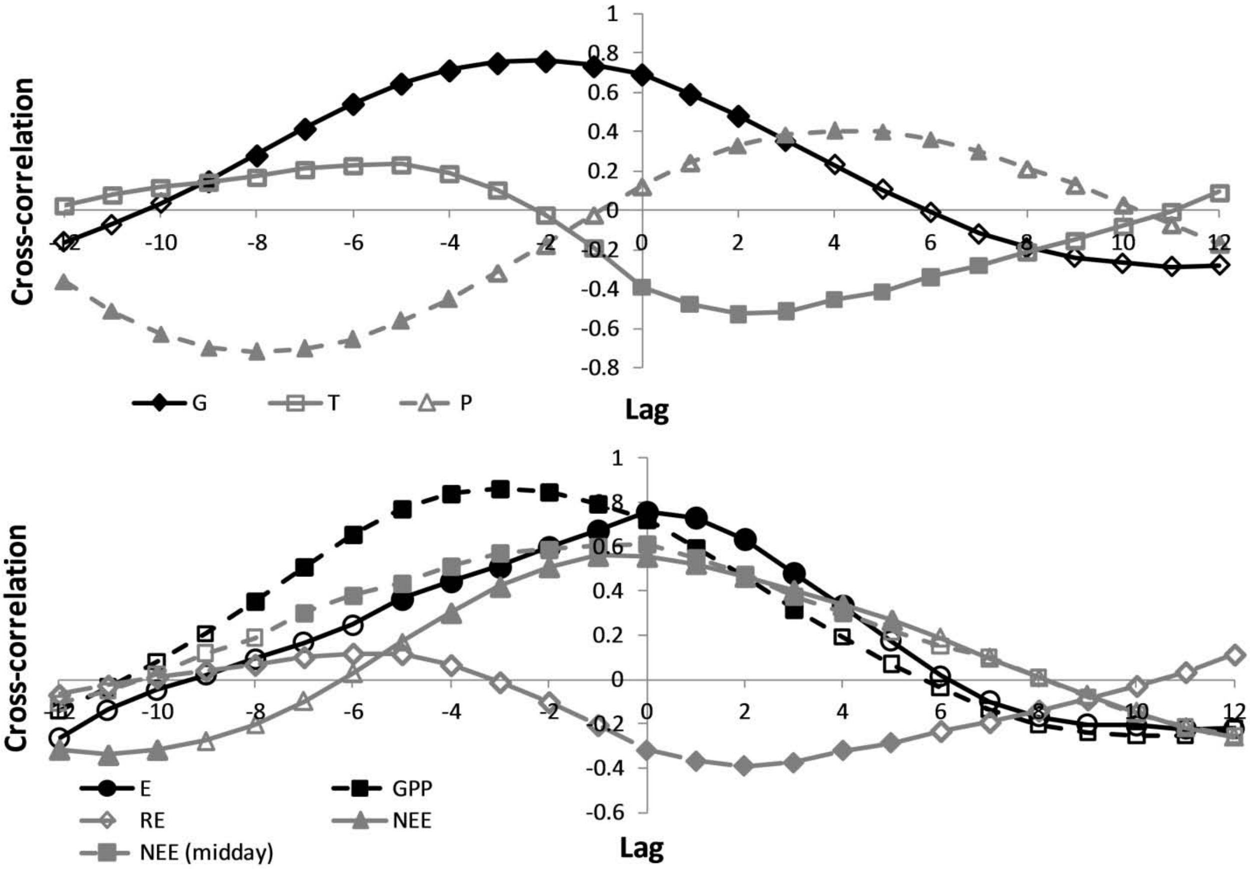

Figure 5. Cross-correlation functions between ΔG_{MA}, ΔT_{MA}, ΔP_{MA}, ΔE_{MA}, ΔGPP_{MA}, ΔRE_{MA}, ΔNEE_{MA} and midday ΔNEE_{MA} values and SST anomalies in Nino4 zone of equatorial Pacific. Filled symbols are corresponded to p-value <0.05 and non-filled symbols - to p>0.05. Lag step is 1 month.

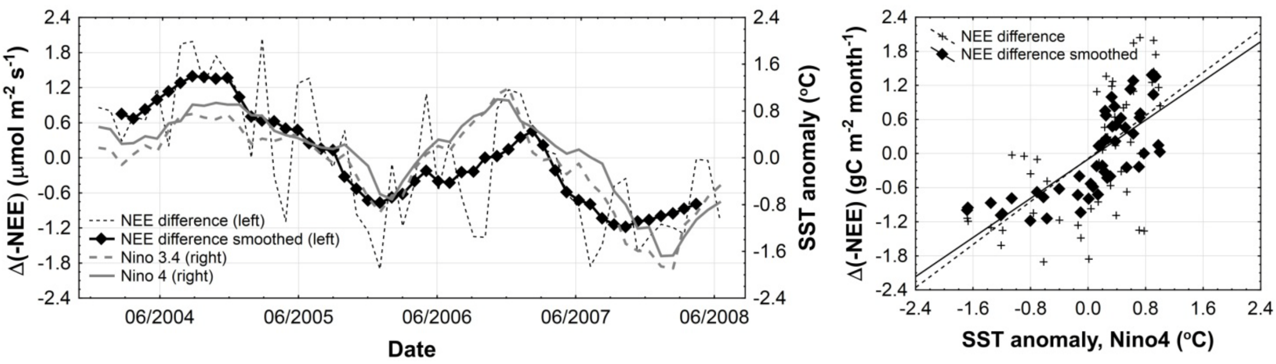

Figure 6. Comparisons of inter-annual pattern of SST anomalies in Nino4 and Nino3.4 zones of equatorial Pacific with variability of both deviations and 7 month (±3 months) moving average deviations of midday NEE (10:00-14:00) values from mean monthly midday values of NEE averaged over the entire measuring period from 2004 to 2008.

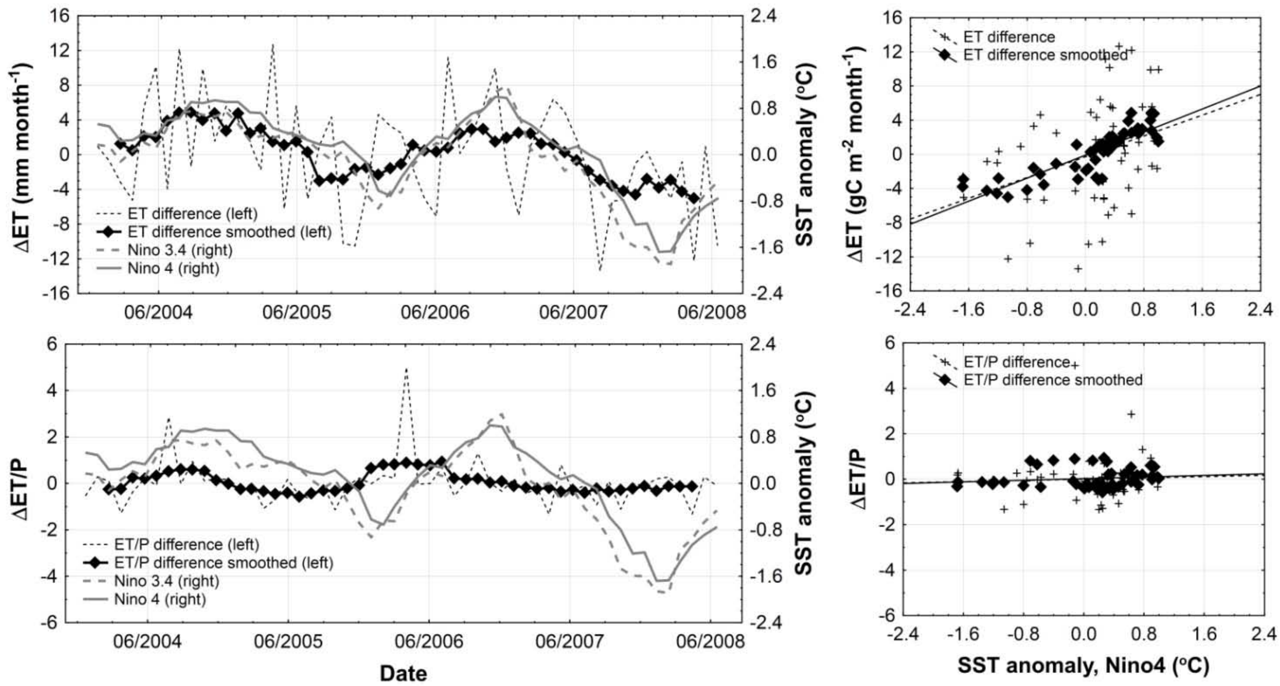

Figure 7. Comparisons of inter-annual pattern of SST anomalies in Nino4 and Nino3.4 zones of equatorial Pacific with variability of both deviations and 7 month (±3 months) moving average deviations of monthly ET rate and ratio ET/P from mean monthly ET rate and ET/P averaged over the entire measuring period from 2004 to 2008.